Inorganica Chimica Acta 387 (2012) 271–276

Contents lists available at SciVerse ScienceDirect

Inorganica Chimica Acta

journal homepage: www.elsevier.com/locate/ica

Six low-dimensional silver(I) coordination complexes derived from 2-aminobenzonitrile and carboxylates

Di Sun [1], Fu-Jing Liu [1], Hong-Jun Hao, Yun-Hua Li, Rong-Bin Huang *, Lan-Sun Zheng

State Key Laboratory for Physical Chemistry of Solid Surfaces and Department of Chemistry, College of Chemistry and Chemical Engineering, Xiamen University, Xiamen 361005, China

ARTICLE INFO

Article history:
Received 26 May 2011
Received in revised form 11 October 2011
Accepted 15 January 2012
Available online 24 January 2012

Keywords:
Silver
2-Aminobenzonitrile
Carboxylate
Crystal structure
Luminescence

ABSTRACT

Six new Ag(I) coordination complexes, $[Ag(abn)(4\text{-cba})]_2$ (**1**), $[Ag(abn)(3\text{-cba})]_2$ (**2**), $[Ag(abn)(fba)]_2$ (**3**), $[Ag(abn)(3\text{-mba})]_2$ (**4**), $[Ag(abn)(moba)]_2$ (**5**), $[Ag(abn)_2(4\text{-mba})]_n$ (**6**), (abn = 2-aminobenzonitrile, 4-cbaH = 4-chlorobenzoic acid, 3-cbaH = 3-chlorobenzoic acid, Hfba = 3-fluorobenzoic acid, 3-mbaH = 3-methylbenzoic acid, Hmoba = 2-methoxybenzoic acid and 4-mbaH = 4-methylbenzoic acid), have been synthesized and characterized by elemental analysis, IR spectra and single crystal X-ray diffraction. Complexes **1–4** are similar discrete binuclear Ag(I) motif containing monodentate μ_1-N_{amino} abn and μ_2-η^1:η^1 carboxylates. The complementary N_{amino}–H···N_{cyano} hydrogen bonds link the binuclear motifs into 1D chain which is further extended into 2D supramolecular sheet by N_{amino}–H···$O_{carboxyl}$ hydrogen bonds. Notably, the electronic effect of substituents in **1–4** has deeply influence on the Ag···Ag interaction. Complex **5** is also a discrete binuclear Ag(I) motif but contains a monodentate μ_1-N_{cyano} abn ligand. The 1D chain was observed in complex **6** where two different abn ligands with μ_1-N_{cyano} and μ_2-N_{cyano}, N_{amino} coordination modes coexist and 4-mba is a chelating μ_1-η^1:η^1 ligand. The results show that the different structures are predominantly attributed to the various ancillary carboxylate ligands and diverse coordination modes of abn ligand. Moreover, the emissive behaviors of them are discussed.

1. Introduction

The construction of hybrid organic–inorganic coordination complexes (CCs) is of high interest in crystal engineering which aims to predict and control the fashion molecules assemble in the solid state [1–4]. In this field, the metal ions and organic ligands, or called nodes and spacers, are of supreme importance in designing CCs with unique properties for a wide range of potential applications including gas storage [5], antimicrobial [6], conductive material [7], luminescent [8], and magnetic materials [9]. Apart from the strong directional metal–ligand bonds, other non-covalent interactions such as hydrogen bonds [10], π···π [11], and d^{10}···d^{10} (aurophilic and argentophilic) interactions [12,13], as well as their combination, also play an important role in supporting the supramolecular solid-state architectures. Among coinage d^{10} metal complexes, Ag(I) CCs have received much attention because Ag(I) shows diverse coordination geometries (linearity, trigon, tetrahedron, square planar square pyramidal and so on) and a propensity of formation of polynuclear Ag(I) aggregations by Ag(I)···Ag(I) interactions [14–18]. On the other hand, N-containing heterocyclic donors (such as pyridine, pyrazine, pyrimidine, and their derivatives) have been widespreadly used in transition metal CCs as either bridging or chelating ligands [19–30], while aminobenzonitrile ligands have attracted less attention from both theoretical and experimental points of view and are rarely used in Ag(I) CCs due to their both weak coordination sites, N_{cyano} and N_{amino} [31]. In our recent work [32], the abn ligands not only afford hydrogen-bonded networks but also lead to the formation of 0D, 1D and 2D CCs due to different coordination preferences such as coordination to the metal centre in monodentate (using either N_{amino} or N_{cyano}), bidentate or bridging fashion (using both N_{amino} and N_{cyano}). With these points in mind, we initiated a project to examine the influence of ancillary carboxylate ligands on Ag/abn assembly system. Herein, we report six new mixed ligands Ag(I)/abn/carboxylate CCs, namely, $[Ag(abn)(4\text{-cba})]_2$ (**1**), $[Ag(abn)(3\text{-cba})]_2$ (**2**), $[Ag(abn)(fba)]_2$ (**3**), $[Ag(abn)(3\text{-mba})]_2$ (**4**), $[Ag(abn)(moba)]_2$ (**5**), $[Ag(abn)_2(4\text{-mba})]_n$ (**6**), (abn = 2-aminobenzonitrile, 4-cbaH = 4-chlorobenzoic acid, 3-cbaH = 3-chlorobenzoic acid, Hfba = 3-fluorobenzoic acid, 3-mbaH = 3-methylbenzoic acid, Hmoba = 2-methoxybenzoic acid and 4-mbaH = 4-methylbenzoic acid) (Scheme 1).

2. Experimental

2.1. Materials and instrumentation

All the reagents and solvents employed were commercially available and used as received without further purification. Infrared spectra were recorded on a Nicolet AVATAT FT-IR330 spectrometer as KBr pellets in the frequency range 4000–400 cm^{-1}. The elemental

* Corresponding author.
E-mail address: rbhuang@xmu.edu.cn (R.-B. Huang).
[1] These authors contributed equally to this work.

0020-1693/$ - see front matter © 2012 Elsevier B.V. All rights reserved.
doi:10.1016/j.ica.2012.01.027

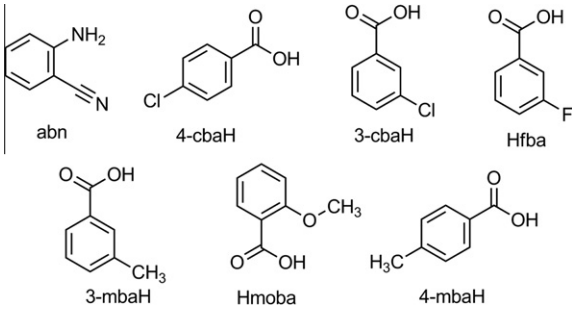

Scheme 1. The organic ligands used in this work.

analyses (C, H, N contents) were determined on a CE instruments EA 1110 analyzer. Photoluminescence measurements were performed on a Hitachi F-7000 fluorescence spectrophotometer with solid powder on a 1 cm quartz round plate.

2.2. Synthesis of complex $[Ag(abn)(4\text{-}cba)]_2$ (**1**)

A mixture of Ag_2O (23 mg, 0.1 mmol), abn (24 mg, 0.2 mmol) and 4-cbaH (31 mg, 0.2 mmol) was stirred in methanol–ethanol mixed solvent (6 mL, *v*/*v*: 1/1). Then aqueous NH_3 solution (25%, 1 mL) was dropped into the mixture to give a clear solution under ultrasonic treatment. The resultant solution was allowed to evaporate slowly in darkness at room temperature for several days to give colorless crystals of **1** (yield: 23%, based on silver), they were washed with a small volume of cold ethanol and dried in air. *Anal.* Calc. for $Ag_2C_{28}H_{20}Cl_2N_4O_4$: C, 44.07; H, 2.64; N, 7.34. Found: C, 42.40; H, 2.37; N, 5.60%. IR (KBr): $\nu(cm^{-1})$ = 3460 (w), 3368 (w), 2210 (w), 1625 (w), 1590 (s), 1545 (s), 1495 (w), 1458 (w), 1400 (s), 1280 (w), 1263 (w), 1099 (m), 1013 (m), 840 (m), 775 (s), 686 (w), 530 (m), 476 (w).

2.3. Synthesis of complex $[Ag(abn)(3\text{-}cba)]_2$ (**2**)

The synthesis of **2** was similar to that of **1**, but with 3-cbaH (31 mg, 0.2 mmol) in place of 4-cbaH. Colorless crystals of **2** were obtained in 35% yield (based on silver). They were washed with a small volume of cold ethanol and dried in air. *Anal.* Calc. for $Ag_2C_{28}H_{20}Cl_2N_4O_4$: C, 44.07; H, 2.64; N, 7.34. Found: C, 43.80; H, 2.59; N, 7.31%. IR (KBr): $\nu(cm^{-1})$ = 3460 (m), 3438 (m), 3368 (m), 3323 (m), 3210 (m), 2208 (m), 1657 (m), 1613 (s), 1601 (s), 1557 (s), 1494 (m), 1459 (w), 1418 (w), 1385 (s), 1313 (w), 1265 (w), 761 (m), 747 (m), 674 (w), 502 (w).

2.4. Synthesis of complex $[Ag(abn)(fba)]_2$ (**3**)

The synthesis of **3** was similar to that of **1**, but with Hfba (28 mg, 0.2 mmol) in place of 4-cbaH. Colorless crystals of **3** were obtained in 33% yield (based on silver). They were washed with a small volume of cold ethanol and dried in air. *Anal.* Calc. for $Ag_2C_{28}H_{20}F_2N_4O_4$: C, 46.05; H, 2.76; N, 7.67. Found: C, 44.08; H, 2.77; N, 6.51%. IR (KBr): $\nu(cm^{-1})$ = 3460 (s), 3368 (s), 2210 (m), 1627 (m), 1598 (m), 1556 (s), 1495 (m), 1458 (m), 1398 (s), 1314 (w), 1267 (m), 1224 (m), 920 (w), 795 (m), 765 (m), 747 (m), 673 (w), 494 (w).

2.5. Synthesis of complex $[Ag(abn)(3\text{-}mba)]_2$ (**4**)

The synthesis of **4** was similar to that of **1**, but with 3-mbaH (27 mg, 0.2 mmol) in place of 4-cbaH. Colorless crystals of **4** were obtained in 34% yield (based on silver). They were washed with a small volume of cold ethanol and dried in air. *Anal.* Calc. for $Ag_2C_{30}H_{26}N_4O_4$: C, 49.89; H, 3.63; N, 7.76. Found: C, 46.99; H, 3.40; N, 5.77%. IR (KBr): $\nu(cm^{-1})$ = 3456 (s), 2212 (w), 1595 (m), 1559 (s), 1494 (w), 1438 (w), 1390 (m), 792 (w), 758 (m), 674 (w), 496 (w).

2.6. Synthesis of complex $[Ag(abn)(moba)]_2$ (**5**)

The synthesis of **5** was similar to that of **1**, but with Hmoba (30 mg, 0.2 mmol) in place of 4-cbaH. Colorless crystals of **5** were obtained in 22% yield (based on silver). They were washed with a small volume of cold ethanol and dried in air. *Anal.* Calc. for $Ag_2C_{30}H_{26}N_4O_6$: C, 47.77; H, 3.47; N, 7.43. Found: C, 46.52; H, 3.08; N, 6.18%. IR (KBr): $\nu(cm^{-1})$ = 3460 (s), 3368 (s), 2210 (w), 1626 (m), 1602 (s), 1588 (s), 1562 (s), 1494 (m), 1457 (m), 1405 (s), 1241 (m), 1101 (w), 1024 (w), 847 (w), 751 (m), 661 (w), 571 (w), 494 (m).

2.7. Synthesis of complex $[Ag(abn)_2(4\text{-}mba)]_n$ (**6**)

The synthesis of **6** was similar to that of **1**, but with 4-mbaH (27 mg, 0.2 mmol) in place of 4-cbaH. Colorless crystals of **6** were obtained in 33% yield (based on silver). They were washed with a small volume of cold ethanol and dried in air. *Anal.* Calc. for $AgC_{22}H_{19}N_4O_2$: C, 55.13; H, 4.00; N, 11.69. Found: C, 53.52; H, 3.46; N, 10.23%. IR (KBr): $\nu(cm^{-1})$ = 3460 (s), 3367 (s), 2209 (m), 1626 (s), 1593 (s), 1550 (s), 1494 (s), 1456 (m), 1402 (m), 1312 (m), 1266 (m), 1156 (w), 847 (w), 762 (m), 746 (m), 493 (m).

3. X-ray crystallography

Single crystals of the CCs **1**–**6** with appropriate dimensions were chosen under an optical microscope and quickly coated with high vacuum grease (Dow Corning Corporation) before being mounted on a glass fiber for data collection. Data for **1**, **4** and **5** were collected on a Bruker-AXS CCD single-crystal diffractometer with graphite-monochromated Mo Kα radiation source (λ = 0.71073 Å). A preliminary orientation matrix and unit cell parameters were determined from 3 runs of 20 frames each, each frame corresponds to a 0.3° scan in 5 s, followed by spot integration and least-squares refinement. Data were measured using ω scans of 0.3° per frame for 10 s until a complete hemisphere had been collected. Cell parameters were retrieved using SMART software and refined with SAINT on all observed reflections [33]. Data reduction was performed with the SAINT software and corrected for Lorentz and polarization effects. Absorption corrections were applied with the program SADABS [33]. Data for **2**, **3** and **6** were collected on a Rigaku R-AXIS RAPID Image Plate single-crystal diffractometer with graphite-monochromated Mo Kα radiation source (λ = 0.71073 Å) operating at 50 kV and 90 mA in ω scan mode. A total of 44 × 5.00° oscillation images was collected, each being exposed for 100 s. The cell refinement and data reduction for them were accomplished with the PROCESS-AUTO processing program [34]. Absorption correction was applied by correction of symmetry-equivalent reflections using the ABSCOR program [35]. In all cases, the highest possible space group was chosen. All structures were solved by direct methods using SHELXS-97 [36] and refined on F^2 by full-matrix least-squares procedures with SHELXL-97 [37]. Atoms were located from iterative examination of difference *F*-maps following least squares refinements of the earlier models. Hydrogen atoms were placed in calculated positions and included as riding atoms with isotropic displacement parameters 1.2–1.5 times U_{eq} of the attached C or N atoms. All structures were examined using the Addsym subroutine of PLATON [38] to assure that no additional symmetry could be applied to the models. The crystallographic details of **1–6** are summarized in Table 1.

Selected bond lengths and angles for **1–6** are collected in Table 2. The hydrogen bond geometries for **1–6** are shown in Table S1.

4. Results and discussion

4.1. Syntheses and IR

The syntheses of complexes **1–6** were carried out in the darkness to avoid photodecomposition. The infrared spectra and elemental analyses of **1–6** are fully consistent with their formations. Their IR spectra (Fig. S1) exhibit absorptions centered at ~3450 and ~3350 cm^{-1} corresponding to asymmetric and symmetric N–H stretching bands of amino group. The peak at ~2210 cm^{-1} can be assigned to the characteristic vibrations of the cyano group. Strong characteristic bands of carboxylic group are observed in the range of ~1600–1560 cm^{-1} for asymmetric vibrations and ~1480 cm^{-1} for symmetric vibrations, respectively.

4.2. Crystal structures

4.2.1. Crystal structure of [Ag(abn)(4-cba)]$_2$ (**1**) [Ag(abn)(3-cba)]$_2$ (**2**), [Ag(abn)(fba)]$_2$ (**3**), [Ag(abn)(3-mba)]$_2$ (**4**)

The results of X-ray crystallographic analysis revealed that complex **1** crystallizes in triclinic $P\bar{1}$ space group. There are one Ag(I) ion, one abn ligand and one 4-cba anion in the asymmetric unit. As illustrated in Fig. 1a, the Ag1 is coordinated by one N atom (N_{amino}) and two O atoms from two different 4-cba ligands, giving a T-shaped coordination geometry [Ag1–N2 = 2.614(3), Ag1–O1 = 2.183(3), Ag1–$O2^i$ = 2.195(2) Å]. The Ag–N bond length in complex **1** is obviously longer than other reported Ag–$N_{heterocycle}$ bond [39–50], which supports the point that the N_{amino} and N_{cyano} atoms are both weaker electron donors compared to $N_{heterocycle}$ atoms. The angles around Ag1 range from 91.16(9)° to 162.49(10)°. The Ag1 also weakly interacts with one N_{cyano} atom with a longer distance of 2.719(3) Å. The Ag–N and Ag–O bond lengths are well-matched with these reported in the related complexes [51]. The dihedral angle between the coordinated carboxyl group and phenyl ring is 19.6(2)°. A pair of symmetry-related Ag(I) ions are clamped by a μ_2-η^1:η^1 carboxyl group, yielding a binuclear Ag(I) motif incorporating a short ligand-supported Ag···Ag contact of 2.8950(9) Å, which is not only well below the sum of van de Walls radii of two Ag ions (3.44 Å) but also very

Table 2
Selected bond distances (Å) and angles (°) for **1–6.**

Complex ***1***			
Ag1–O1	2.183(3)	Ag1–N2	2.614(3)
Ag1–$O2^i$	2.195(2)	Ag1–$Ag1^i$	2.8950(9)
O1–Ag1–$O2^i$	162.49(10)	$O2^i$–Ag1–N2	91.16(9)
O1–Ag1–N2	102.80(9)		
Symmetry code: (i) $-x, -y+1, -z+1$			
Complex ***2***			
Ag1–O1	2.194(6)	Ag1–N1	2.624(7)
Ag1–$O2^i$	2.202(6)	Ag1–$Ag1^i$	2.9329(16)
O1–Ag1–$O2^i$	162.1(2)	$O2^i$–Ag1–N1	90.7(2)
O1–Ag1–N1	103.5(2)		
Symmetry code: (i) $-x+1, -y+1, -z+1$			
Complex ***3***			
Ag1–$O2^i$	2.189(3)	Ag1–N1	2.658(4)
Ag1–O1	2.205(3)	Ag1–$Ag1^i$	2.9290(9)
$O2^i$–Ag1–O1	161.92(11)	O1–Ag1–N1	90.90(12)
$O2^i$–Ag1–N1	102.90(12)		
Symmetry code: (i) $-x+2, -y+1, -z$			
Complex ***4***			
Ag1–$O2^i$	2.175(3)	Ag1–N1	2.649(3)
Ag1–O1	2.185(3)	Ag1–$Ag1^i$	2.8755(12)
$O2^i$–Ag1–O1	162.94(10)	O1–Ag1–N1	92.06(10)
$O2^i$–Ag1–N1	101.60(10)		
Symmetry code: (i) $-x+1, -y+1, -z+1$			
Complex ***5***			
Ag1–O1	2.215(7)	Ag1–N2	2.394(9)
Ag1–$O2^i$	2.222(7)	Ag1–$Ag1^i$	2.8080(18)
O1–Ag1–$O2^i$	164.9(3)	$O2^i$–Ag1–N2	87.6(3)
O1–Ag1–N2	107.2(3)		
Symmetry code: (i) $-x, -y+2, -z+1$			
Complex ***6***			
Ag1–N3	2.317(5)	Ag1–O1	2.343(3)
Ag1–$N4^i$	2.320(4)	Ag1–N1	2.385(5)
Ag1–O2	2.671(3)		
N3–Ag1–$N4^i$	96.05(16)	N3–Ag1–N1	104.30(17)
N3–Ag1–O1	110.10(15)	$N4^i$–Ag1–N1	107.03(17)
$N4^i$–Ag1–O1	142.15(13)	O1–Ag1–N1	92.85(16)
Symmetry code: (i) $x, y+1, z$			

Table 1
Crystallographic data for complexes **1–6.**

Complexes	**1**	**2**	**3**	**4**	**5**	**6**
Formula	$C_{28}H_{20}Ag_2Cl_2N_4O_4$	$C_{28}H_{20}Ag_2Cl_2N_4O_4$	$C_{28}H_{20}Ag_2F_2N_4O_4$	$C_{30}H_{26}Ag_2N_4O_4$	$C_{30}H_{26}Ag_2N_4O_6$	$C_{22}H_{19}AgN_4O_2$
M_r	763.12	763.12	730.22	722.29	754.29	479.28
Crystal system	triclinic	triclinic	monoclinic	triclinic	monoclinic	monoclinic
Space group	$P\bar{1}$	$P\bar{1}$	$P2_1/c$	$P\bar{1}$	$P2_1/c$	$P2_1/c$
a (Å)	4.2634(11)	4.2789(9)	4.2217(8)	4.3152(17)	9.7284(19)	15.131(4)
b (Å)	10.327(3)	10.393(2)	28.494(6)	10.343(4)	5.8347(12)	6.3211(15)
c (Å)	15.565(4)	15.245(3)	10.512(2)	15.212(6)	24.369(5)	22.121(5)
α (°)	80.474(4)	75.00(3)	90.00	74.669(7)	90.00	90.00
β (°)	83.313(4)	84.42(3)	92.96(3)	83.260(6)	96.86(3)	105.984(4)
γ (°)	87.119(4)	87.03(3)	90.00	86.014(7)	90.00	90.00
Z	1	1	2	1	2	4
V (Å^3)	670.9(3)	651.5(2)	1262.8(4)	649.7(4)	1373.3(5)	2034.0(8)
D_c (g cm^{-3})	1.889	1.945	1.920	1.846	1.824	1.565
μ (mm^{-1})	1.702	1.753	1.610	1.553	1.479	1.016
F(000)	376	376	720	360	752	968
No. of unique reflections	2267	2270	2208	2209	2393	3584
No. of observed reflections [$I > 2\sigma(I)$]	2220	1438	2056	2093	1414	2909
Parameters	181	182	181	182	192	263
GOF	1.097	1.074	1.170	1.076	1.108	1.041
Final R indices [$I > 2\sigma(I)$][a,b]	R_1 = 0.0340	R_1 = 0.0628	R_1 = 0.0372	R_1 = 0.0352	R_1 = 0.0624	R_1 = 0.0537
	wR_2 = 0.0908	wR_2 = 0.1198	wR_2 = 0.0892	wR_2 = 0.0919	wR_2 = 0.1287	wR_2 = 0.1229
R indices (all data)	R_1 = 0.0347	R_1 = 0.1116	R_1 = 0.0400	R_1 = 0.0372	R_1 = 0.1173	R_1 = 0.0679
	wR_2 = 0.0915	wR_2 = 0.1535	wR_2 = 0.0931	wR_2 = 0.0934	wR_2 = 0.1846	wR_2 = 0.1302
Largest difference peak and hole (e Å^{-3})	0.884 and −0.547	0.863 and −1.376	0.756 and −0.736	1.039 and −0.517	1.241 and −1.486	0.694 and −0.470

[a] $R_1 = \sum||F_o| - |F_c||/\sum|F_o|$.
[b] $wR_2 = [\sum w(F_o^2 - F_c^2)^2/\sum w(F_o^2)^2]^{0.5}$.

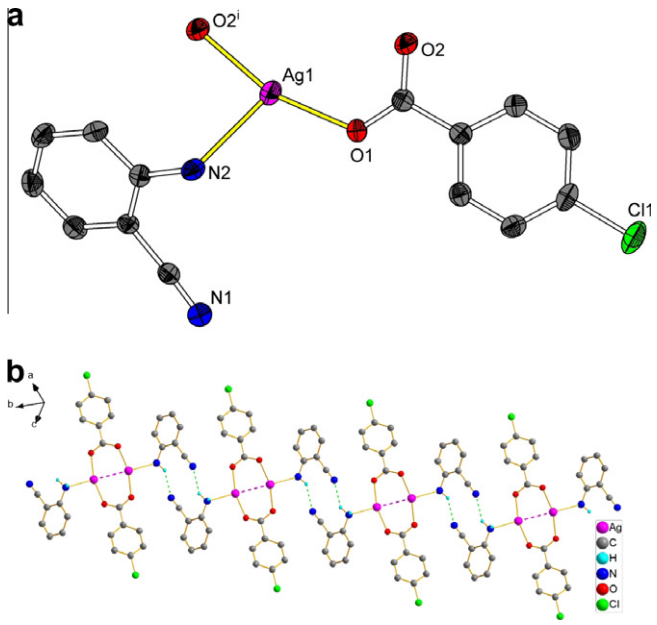

Fig. 1. (a) The coordination environments of the Ag(I) centers and the linkage modes of ligands in **1** with 50% thermal ellipsoid probability. Hydrogen atoms are omitted for clarity. (b) A ball and stick diagram showing the one-dimensional chain incorporating complementary N_{amino}–H···N_{cyano} hydrogen bond (green dashed line) (symmetry code: (i) $-x$, $-y+1$, $-z+1$). (For interpretation of the references to colour in this figure legend, the reader is referred to the web version of this article.)

close to the Ag···Ag distance in metal silver (2.89 Å) [52], suggesting significant argentophilic interaction [53–57] (symmetry code: (i) $-x$, $-y+1$, $-z+1$).

The complementary N_{amino}–H···N_{cyano} hydrogen bonds (N2–H2B···N1^{ii} = 3.045(4) Å) link the binuclear motifs into 1D chain (Fig. 1b and Table S1) which is further extended into 2D supramolecular sheet by N_{amino}–H···$O_{carboxyl}$ hydrogen bonds (N2–H2C···O2^{iii} = 2.901(4) Å). The non-classic C–H···Cl hydrogen bond (3.571(4) Å) contributes to the stability of the molecules packing in the crystal (symmetry codes: (ii) $-x-1$, $-y$, $-z+1$; (iii) $-x-1$, $-y+1$, $-z+1$).

Both the basic structures and molecules packing of complexes **2**–**4** are similar to those of **1** (Fig. S2). The Ag–N and Ag–O bond lengths of them are in the ranges of 2.624(7)–2.658(4) Å and 2.175(3)–2.205(3) Å, respectively. The dihedral angles between the coordinated carboxyl group and phenyl ring in **2**–**4** are 18.5(2)°, 18.1(2)° and 19.3(2)°, respectively. From the structural analysis of **1**–**4**, we can see that the presence of different electron withdrawing or donating substituents on the benzoic acid surprisingly do not change structure motifs intrinsically which give us an opportunity to investigate the influence of substituents on the Ag···Ag interactions by structural comparison of these complexes. The coordination modes of both abn and carboxylate ligands are identical in **1**–**4** but the Ag···Ag distances are slightly different which is caused by the different electronic effects of substituents. As we know, the closed-shell argentophilic interaction is weak attractive force in nature [58] and is often gainfully exploited in constructing a wide array of extended supramolecular networks in designing materials [59]. The Ag···Ag distances in complexes **1**–**4** are 2.8950(9), 2.9329(16), 2.9291(9) and 2.8755(12) Å, respectively. Compared to electron withdrawing halogen (F and Cl) substituents in **1**–**3**, the methyl is an electron donating group in **4** which pushes its σ electrons toward the aromatic phenyl ring, as

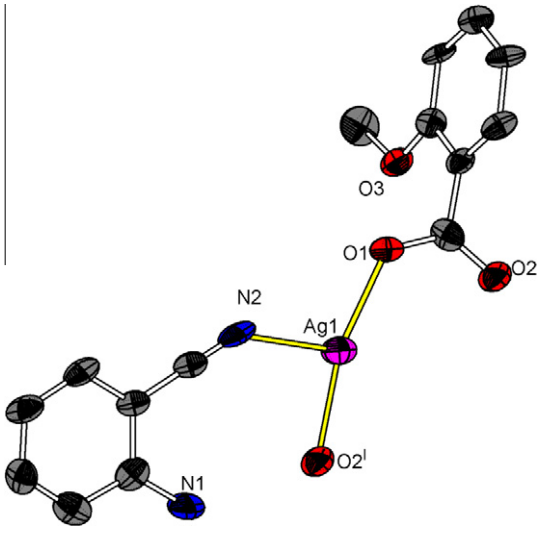

Fig. 2. A 50% thermal ellipsoid representation of coordination environment of Ag(I) ion in **5**. Hydrogen atoms are omitted for clarity (symmetry code: (i) $-x$, $-y+2$, $-z+1$).

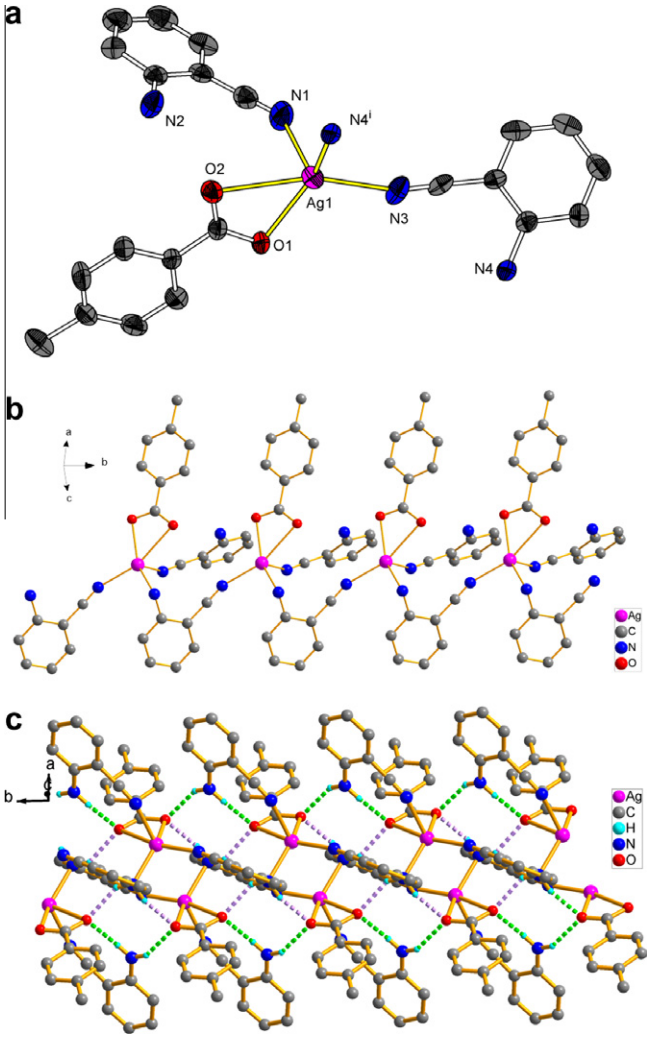

Fig. 3. (a) The coordination environments of the Ag(I) centers and the linkage modes of ligands in **6** with 50% thermal ellipsoid probability. Hydrogen atoms are omitted for clarity. (b) A ball and stick diagram showing the one-dimensional chain. (c) A ball and stick diagram showing one-dimensional double chain incorporating intrachain (green dashed line) and interchain (purple dashed line) hydrogen bonds (symmetry code: (i) x, $y+1$, z). (For interpretation of the references to colour in this figure legend, the reader is referred to the web version of this article.)

Table 3
A comparison of the structural features for complexes **1–6.**

Complex (R)	abn	Carboxylate	Structure motif	Ag···Ag distance
1 (4-Chloro)	μ_1-N_{amino}	μ_2-η^1:η^1	0D binuclear	2.8950(9)
2 (3-Chloro)	μ_1-N_{amino}	μ_2-η^1:η^1	0D binuclear	2.9329(16)
3 (3-Fluoro)	μ_1-N_{amino}	μ_2-η^1:η^1	0D binuclear	2.9291(9)
4 (3-methyl)	μ_1-N_{amino}	μ_2-η^1:η^1	0D binuclear	2.8755(12)
5 (2-Methoxy)	μ_1-N_{cyano}	μ_2-η^1:η^1	0D binuclear	2.8080(18)
6 (4-Methyl)	μ_1-N_{cyano} and μ_2-N_{cyano}, N_{amino}	μ_1-η^1:η^1	1D chain	No

a consequence, the electron density on the coordinated carboxyl group is increased through a inductive effect and the repel force between a pair of neighboring positive Ag(I) ions is decreased, giving the shorter Ag···Ag distance.

*4.2.2. Crystal structure of [Ag(abn)(moba)]$_2$ (**5**)*

When carboxylate is replaced by Hmoba, a similar binuclear Ag(I) structure is formed. The asymmetry unit of **5** consists one Ag(I) ion, one abn ligand and one moba anion. As shown in Fig. 2, the Ag(I) center features a T-shaped geometry completed by one N atom (N_{cyano}) and two O atoms from two distinct moba ligands [Ag1–O1 = 2.215(7), Ag1–O2^i = 2.222(7), Ag1–N2 = 2.394(9) Å] without consideration of Ag···Ag interactions. The weak Ag···N_{amino} and Ag···O interactions give distances of 3.224(9) and 3.155(7) Å, respectively. These separations are a little longer but still fall in the secondary bonding range (the sums of Van der Waals radii of Ag and N, Ag and O are 3.27 and 3.24 Å, respectively). The dihedral angle between the coordinated carboxyl group and phenyl ring is 69.4(2)° in **5** and much larger than the average values (18.9(2)°) for **1–4,** indicating the significantly steric effect of methoxyl group. In contrary to the consentaneously monodentate coordinated amino group of abn in **1–4**, it is also noteworthy that the coordination site of abn is changed to N atom of cyano group in **5**. In this binuclear motif, a short Ag···Ag interaction (2.8080(18) Å) and intramolecular N–H···O hydrogen bond (2.936(11) Å) are observed (symmetry code: (i) $-x$, $-y+2$, $-z+1$).

*4.2.3. Crystal structure of [Ag(abn)$_2$(4-mba)]$_n$ (**6**)*

When 3-mba in **4** is replaced by its isomer 4-mba, a 1D chain structure is obtained. The asymmetry unit of **6** consists one Ag(I) ion, two abn ligand and one 4-mba anion. As shown in Fig. 3a, the Ag1 adopts a distorted square pyramidal coordination geometry by coordinating with three N atoms from three different abn ligands and two O atoms from the same 4-mba anion (Ag1–N3 = 2.317(5), Ag1–N4^i = 2.320(4), Ag1–N1 = 2.385(5), Ag1–O1 = 2.343(3) and Ag1–O2 = 2.671(3) Å). The distortion of the trigonal bipyramidal geometry can be indicated by the calculated value of the τ_5 parameter introduced by Addison [60] to describe the geometry of a five-coordinated metal system, which is 0.32 for Ag1, indicating that the Ag1 locates in a distorted square pyramidal geometry (for a trigonal bipyramidal structure with D_{3h} symmetry, $\tau_5 = 1$, then for a square pyramidal structure with C_{4v} symmetry, $\tau_5 = 0$). In complex **6**, abn ligands show two kinds of coordination modes, μ_1-N_{cyano} and μ_2-N_{cyano}, N_{amino}, respectively. The μ_2-N_{cyano}, N_{amino} abn bridges Ag(I) ions into 1D chain along the *b* axis (Fig. 3b). The bidentate chelating 4-mba and μ_1-N_{cyano} abn do not attribute to the extension of the 1D chain (symmetry code: (i) x, $y+1$, z).

The uncoordinated amino groups of μ_1-N_{cyano} abn form the intrachain hydrogen bond with carboxyl groups of 4-mba to consolidate the 1D chain. Furthermore, the coordinated amino groups of μ_2-N_{cyano}, N_{amino} abn are hydrogen bonded to the 4-mba from adjacent chain, resulting the 1D supramolecular double chain structure. According to graphset analysis nomenclature, the intra- and interchain hydrogen bonds form a $R_4^2(8)$ hydrogen motif [61] within the 1D double chain.

*4.3. Structural comparison for complexes **1–6***

In spite of all the Ag(I) complexes **1–6** were synthesized under the same condition by using similar organic ligands, different structures are observed, which can be properly ascribed to the substituent effects (position and electronic effects) of benzoic acid ligand [62]. A detailed comparison of their structural features is summarized in Table 3. Complexes **1–5** are similar binuclear Ag(I) motifs, but the significant differences, such as different Ag···Ag distances and coordination modes of abn ligand, were worthy to note. For **1–5**, when the substituents change from electron withdrawing halogens (F and Cl) to electron donating group (CH_3– and CH_3O–), the basic binuclear Ag(I) motif keeps silent, but the Ag···Ag distances vary from 2.9329(16) to 2.8080(18) Å which not only indicate the electronic effect of substituents has important impact on the argentophilic interaction but also validate the essence of the argentophilic interaction. Generally speaking, argentophilic interaction is intrinsically weak attractive force, so electron donating substituent can effectively diminish repel force between pairs of Ag(I) ions, giving the shorter Ag···Ag distance, compared to the electron withdrawing substituent. For example, the methoxyl group in **5** has the strongest electron donating ability in this system, as a result, the shortest Ag···Ag distance appears. For **4** and **6**, different positions of methyl group on benzoic acid influence the coordination modes of abn as well as carboxylates, consequently, control the dimensionalities (0D and 1D) of them.

4.4. Photoluminescence properties

The photoluminescence properties of **1–6** were examined in the solid state at room temperature as shown in Fig. 4. The intense

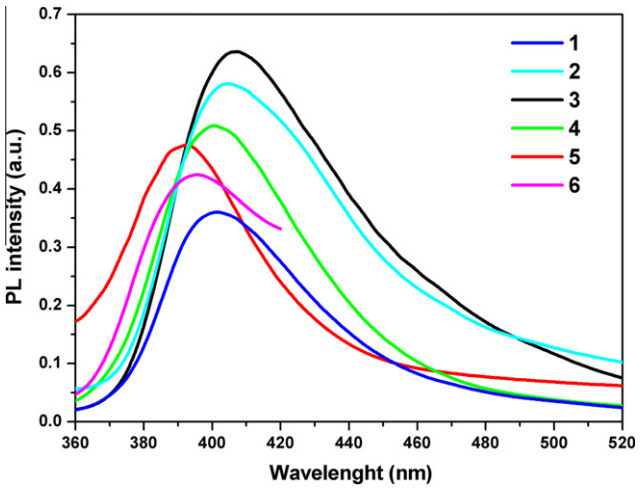

Fig. 4. Emission spectra of the complexes **1–6.**

emission bands are observed at 400 nm for **1**, 404 nm for **2**, 407 nm for **3**, 401 nm for **4**, 392 nm for **5** and 395 nm for **6** at room temperature (λ_{ex} = 300 nm). The abn displays photoluminescent emissions at 408 nm under 300 nm radiation which are probably attributed to the $\pi^* \rightarrow \pi$ transitions [32]. All emission bands for **1–6** locate around 400 nm which are similar to the emission of abn ligand. So the photoluminescence of **1–6** should originate from the transitions between the energy levels of the abn ligand [63,64]. Because the conjugated system of organic ligand is similar with each other, the arrangement of organic ligand and different Ag···Ag interaction may be responsible to the different emissions of **1–6**.

5. Conclusions

To further demonstrate the influence of substituents for benzoic acid in constructing coordination architectures, in this work, we synthesized and characterized six low-dimensional mixed ligands CCs ranging from 0D binuclear motifs to 1D chain. The results demonstrated that substituent groups deeply influence not only the basic structures but also some kind of secondary interactions. In addition, the abn ligand and carboxylates display the self-adjusting nature to show different binding fashions upon metalation. The significant substituent effects including positional, electronic and steric effects discovered herein will provide further insights into the rational design and preparation of coordination polymers in future. Moreover, the emissive behaviors of **1–6** were discussed.

Acknowledgments

This work was financially supported by the National Natural Science Foundation of China (Nos. 21021061 and 21071118), 973 Project (Grant 2007CB815301) from MSTC.

Appendix A. Supplementary material

CCDC 824711–824716 contain the supplementary crystallographic data for **1–6** this paper. These data can be obtained free of charge from The Cambridge Crystallographic Data Centre via www.ccdc.cam.ac.uk/data_request/cif. Supplementary data associated with this article can be found, in the online version, at doi:10.1016/j.ica.2012.01.027.

References

[1] J.J. Perry, J.A. Perman, M.J. Zaworotko, Chem. Soc. Rev. 38 (2009) 1400.
[2] S.R. Batten, R. Robson, Angew. Chem., Int. Ed. 37 (1998) 1460.
[3] B. Chen, S. Xiang, G. Qian, Acc. Chem. Res. 43 (2010) 1115.
[4] R. Robson, J. Chem. Soc., Dalton Trans. (2000) 3735.
[5] J.P. Zhang, S. Kitagawa, J. Am. Chem. Soc. 130 (2008) 907.
[6] N.C. Kasuga, A. Sugie, K. Nomiya, Dalton Trans. 21 (2004) 3732.
[7] D. Sun, C.-F. Yang, H.-R. Xu, H.-X. Zhao, Z.-H. Wei, N. Zhang, L.-J. Yu, R.-B. Huang, L.-S. Zheng, Chem. Commun. 46 (2010) 8168.
[8] D. Sun, D.-F. Wang, X.-G. Han, N. Zhang, R.-B. Huang, L.-S. Zheng, Chem. Commun. 47 (2011) 746.
[9] B. Moulton, J.J. Lu, R. Hajndl, S. Hariharan, M.J. Zaworotko, Angew. Chem., Int. Ed. 41 (2002) 2821.
[10] B. Li, R.-J. Wei, J. Tao, R.-B. Huang, L.-S. Zheng, Z. Zheng, J. Am. Chem. Soc. 132 (2010) 15583.
[11] C. Janiak, J. Chem. Soc., Dalton Trans. 12 (2000) 3885.
[12] H. Schmidbaur, Chem. Soc. Rev. 24 (1995) 391.
[13] M.J. Katz, K. Sakai, D.B. Leznoff, Chem. Soc. Rev. 37 (2008) 1884.
[14] Y.-P. Xie, T.C.W. Mak, J. Am. Chem. Soc. 133 (2011) 3760.
[15] G.G. Gao, P.-S. Cheng, T.C.W. Mak, J. Am. Chem. Soc. 131 (2009) 18257.
[16] D. Sun, G.-G. Luo, N. Zhang, Q.-J. Xu, R.-B. Huang, L.-S. Zheng, Polyhedron 29 (2010) 1243.
[17] D. Sun, G.G. Luo, N. Zhang, R.B. Huang, L.S. Zheng, Chem. Commun. 47 (2011) 1461.
[18] D. Sun, Z.-H. Wei, C.-F. Yang, N. Zhang, R.-B. Huang, L.-S. Zheng, Inorg. Chem. Commun. 13 (2010) 1191.
[19] D. Sun, G.G. Luo, R.B. Huang, N. Zhang, L.S. Zheng, Acta Crystallogr., Sect. C 65 (2009) m305.
[20] D. Sun, G.G. Luo, N. Zhang, J.H. Chen, R.B. Huang, L.R. Lin, L.S. Zheng, Polyhedron 28 (2009) 2983.
[21] D. Sun, G.G. Luo, N. Zhang, R.B. Huang, L.S. Zheng, Acta Crystallogr., Sect. C 65 (2009) m418.
[22] D. Sun, G.G. Luo, N. Zhang, R.B. Huang, L.S. Zheng, Acta Crystallogr., Sect. C 65 (2009) m440.
[23] D. Sun, G.G. Luo, N. Zhang, Q.J. Xu, C.F. Yang, Z.H. Wei, Y.C. Jin, L.R. Lin, R.B. Huang, L.S. Zheng, Inorg. Chem. Commun. 13 (2010) 290.
[24] D. Sun, N. Zhang, R.-B. Huang, L.-S. Zheng, Cryst. Growth Des. 10 (2010) 3699.
[25] D. Sun, G.G. Luo, N. Zhang, Z.H. Wei, C.F. Yang, Q.J. Xu, R.B. Huang, L.S. Zheng, J. Mol. Struct. 967 (2010) 147.
[26] D. Sun, H.-R. Xu, C.-F. Yang, Z.-H. Wei, N. Zhang, R.-B. Huang, L.-S. Zheng, Cryst. Growth Des. 10 (2010) 4642.
[27] C.-Y. Lin, Z.-K. Chan, C.-W. Yeh, C.-J. Wu, J.-D. Chen, J.-C. Wang, CrystEngComm 8 (2006) 841.
[28] Y.-H. Wang, K.-L. Chu, H.-C. Chen, C.-W. Yeh, Z.-K. Chan, M.-C. Suen, J.-D. Chen, CrystEngComm 8 (2006) 84.
[29] D. Sun, G.-G. Luo, N. Zhang, Q.-J. Xu, Y.-C. Jin, Z.-H. Wei, C.-F. Yang, L.-R. Lin, R.-B. Huang, L.-S. Zheng, Inorg. Chem. Commun. 13 (2010) 306.
[30] D. Sun, Q.-J. Xu, C.-Y. Ma, N. Zhang, R.-B. Huang, L.-S. Zheng, CrystEngComm 12 (2010) 4161.
[31] D. Sun, Z.H. Wei, C.F. Yang, D.F. Wang, N. Zhang, R.-B. Huang, N. Zhang, L.-S. Zheng, CrystEngComm 13 (2011) 1591.
[32] F.-J. Liu, J. Mol. Struct. 990 (2011) 158.
[33] Bruker, SMART, SAINT and SADABS, Bruker AXS Inc., Madison, Wisconsin, USA, 1998.
[34] Rigaku, PROCESS-AUTO, Rigaku Corporation, Tokyo, Japan, 2004.
[35] T. Higashi, ABSCOR, Empirical Absorption Correction Based on Fourier Series Approximation, Rigaku Corporation, Tokyo, Japan, 1995.
[36] G.M. Sheldrick, SHELXS-97, Program for X-ray Crystal Structure Determination, University of Gottingen, Germany, 1997.
[37] G.M. Sheldrick, SHELXL-97, Program for X-ray Crystal Structure Refinement, University of Gottingen, Germany, 1997.
[38] A.L. Spek, Implemented as the PLATON Procedure, a Multipurpose Crystallographic Tool, Utrecht University, Utrecht, The Netherlands, 1998.
[39] K.V. Domasevitch, P.V. Solntsev, I.A. Gural'skiy, H. Krautscheid, E.B. Rusanov, A.N. Chernega, J.A.K. Howard, Dalton Trans. (2007) 3893.
[40] I.A. Gural'skiy, D. Escudero, A. Frontera, P.V. Solntsev, E.B. Rusanov, A.N. Chernega, H. Krautscheid, K.V. Domasevitch, Dalton Trans. (2009) 2856.
[41] A.S. Degtyarenko, P.V. Solntsev, H. Krautscheid, E.B. Rusanov, A.N. Chernega, K.V. Domasevitch, New J. Chem. 32 (2008) 1910.
[42] H.C. Chen, H.L. Hu, Z.K. Chan, C.W. Yeh, H.W. Jia, C.P. Wu, J.D. Chen, J.C. Wang, Cryst. Growth Des. 7 (2007) 698.
[43] C.W. Yeh, T.R. Chen, J.D. Chen, J.C. Wang, Cryst. Growth Des. 9 (2009) 2595.
[44] C.Y. Lin, Z.K. Chan, C.W. Yeh, C.J. Wu, J.D. Chen, J.C. Wang, CrystEngComm 8 (2006) 841.
[45] X. Wang, J. Feng, J. Huang, J. Zhang, M. Pan, C.-Y. Su, CrystEngComm 12 (2010) 725.
[46] K.M. Park, J. Seo, S.H. Moon, S.S. Lee, Cryst. Growth Des. 10 (2010) 4148.
[47] E. Guney, V.T. Yilmaz, O. Buyukgungor, Polyhedron 29 (2010) 1437.
[48] V.T. Yilmaz, E. Soyer, O. Buyukgungor, Polyhedron 29 (2010) 920.
[49] V.T. Yilmaz, S. Hamamci, S. Gumus, O. Buyukgungor, J. Mol. Struct. 794 (2006) 142.
[50] S. Hamamci, V.T. Yilmaz, W.T.A. Harrison, J. Mol. Struct. 734 (2005) 191.
[51] A. Glees, U. Ruschewitz, Z. Anorg. Allg. Chem. (2009) 2046.
[52] A.J. Bondi, Phys. Chem. 68 (1964) 411.
[53] C.-M. Che, M.-C. Tse, M.C.W. Chan, K.-K. Cheung, D.L. Phillips, K.-H. Leung, J. Am. Chem. Soc. 122 (2000) 2464.
[54] C.Y. Chen, J.Y. Zeng, H.M. Lee, Inorg. Chim. Acta 360 (2007) 21.
[55] X. Liu, G.-C. Guo, M.-L. Fu, X.-H. Liu, M.-S. Wang, J.-S. Huang, Inorg. Chem. 45 (2006) 3679.
[56] L. Dobrzanska, H.G. Raubenheimer, L.J. Barbour, Chem. Commun. (2005) 5050.
[57] A.A. Mohamed, L.M. Pérez, J.P. Fackler Jr., Inorg. Chim. Acta 358 (2005) 1657.
[58] L. Ray, M.M. Shaikh, P. Ghosh, Inorg. Chem. 47 (2008) 230.
[59] A. Burini, A.A. Mohamed, J.P. Fackler Jr., Comments Inorg. Chem. 24 (2003) 253.
[60] A.W. Addison, T.N. Rao, J. Reedijk, J. van Rijn, G.C. Verschoor, J. Chem. Soc., Dalton Trans. (1984) 1349.
[61] J. Bernstein, R.E. Davis, L. Shimoni, N.L. Chang, Angew. Chem., Int. Ed. Engl. 35 (1995) 1555.
[62] J. Chen, C.-P. Li, M. Du, CrystEngComm 13 (2011) 1885.
[63] F.-F. Li, J.-F. Ma, J. Yang, H.-Q. Jia, N.-H. Hu, J. Mol. Struct. 787 (2006) 106.
[64] V.W.W. Yam, Acc. Chem. Res. 35 (2002) 555.